NANO · MICRO small
www.small-journal.com

Supramolecular Assembly with Near-Infrared Emission for Two-Photon Mitochondrial Targeted Imaging

*Fang-Fang Shen, Yong Chen, Xiufang Xu, Hua-Jiang Yu, Haoran Wang, and Yu Liu**

Two-photon supramolecular assembly with near-infrared (NIR) fluorescence emission is constructed from tetraphenylethene derivative possessing methoxyl and vinyl pyridine salt (TPE-2SP), cucurbit[8]uril (CB[8]), and β-cyclodextrin modified hyaluronic acid (HA-CD). The obtained experimental results indicate that the TPE-2SP exhibits a very weak fluorescence emission at 650 nm, and then complexes with cucurbit[7]uril (CB[7]) to form 1:2 supramolecular pseudorotaxane with an enhanced NIR fluorescence emission at 660 nm. Compared with CB[7], CB[8] can assemble with TPE-2SP to be two-axial netlike pseudopolyrotaxane, resulting in close packing to increase TPE-2SP fluorescence emission with a redshift of 30 nm. Interestingly, TPE-2SP/CB[8] continues to assemble with cancer cell targeting agent HA-CD into nanoparticles, leading to assembling-induced further enhancement of NIR emission. Surprisingly, supramolecular nanoparticles have the two-photon character, and are successfully applied to mitochondrial targeting imaging. This supramolecular assembly system, with two-photon absorption and assembly-induced enhanced NIR luminescence properties, opens new way for biological targeted imaging.

1. Introduction

Aggregation-induced emission (AIE) has become an extremely hot research field since it first put forward by Tang et al. in 2001.[1] Benefiting from the advantages of high emission efficiency in aggregates, excellent photostability and large stokes' shift, aggregation-induced emission fluorogens (AIEgens) have been applied in various areas such as organic light-emitting devices, chemical sensors, and bioimaging.[2–4] Among the existing AIEgens, tetra-phenylethene (TPE) as a representative AIE-active molecule has attracted widespread attention and interest because of its simple synthesis, easy modification, and excellent luminous performance.[5] Recently, the luminescent behaviors of TPE derivatives induced by macrocyclic host compounds such as cyclodextrins, cucurbiturils, calixarenes, and pillararenes based on the restriction of intramolecular motion (RIM) mechanism have extremely promoted the AIE development, and successfully been applied in cell imaging and photodynamic therapy.[6,7] Therefore, supramolecular strategy including assembling-induced emission and host–guest induced emission based on macrocyclic host compounds not only expanded the scope of application of AIE,[8] but also contributed to the development of supramolecular chemistry in the fields of materials and biology.[9–11]

Although a lot of efforts have been contributed to supramolecular macrocycle host compounds inducing the emission of guest molecules, including but not limited to AIEgens, most of them showed short absorption or emission wavelengths, [12,13] greatly limiting their application in the biological field. On the other hand, the advantages of two-photon excitation are that most of them are located in the near-infrared region, which can penetrate deeply into the tissue, minimize background interference, improve the imaging signal-to-noise ratio, and avoid the absorption of proteins in the body compared to one-photon excitation. [14–16] However, the construction of supramolecular assembly with both NIR emission and two-photon excitation is very rarely reported.

Herein, we report a two-photon supramolecular ternary assembly with NIR fluorescence emission, which can be used for mitochondrial targeted imaging of A549 cells (**Scheme 1**). This supramolecular ternary assembly was composed of tetraphenylethene derivative with methoxyl and vinyl pyridine salt (TPE-2SP), cucurbit[8]uril (CB[8]), and β-cyclodextrin modified hyaluronic acid (HA-CD). TPE-2SP has an extremely weak fluorescence emission at 650 nm in aqueous solution. After interacting with CB[7], the TPE-2SP emission was strengthened and redshifted to 660 nm. As comparison, the emission of TPE-2SP was enhanced and redshifted to 680 nm after assembling with CB[8] to form nanosquares in aqueous solution. Interestingly, the introduction of the cancer cell targeting agent HA-CD into TPE-2SP/CB[8] can be assembled into nanoparticles via secondary assembly with further enhancement of NIR emission. Surprisingly, such supramolecular nanoparticles with NIR emission having two-photon excitation were successfully applied for mitochondrial targeted cell imaging of A549 cancer cells.

2. Results and Discussion

The detailed synthesis method and characterization data of TPE derivative (TPE-2SP) are summarized. (Figures S1–S4,

F.-F. Shen, Prof. Y. Chen, Prof. X. Xu, H.-J. Yu, H. Wang, Prof. Y. Liu
Department College of Chemistry
Nankai University
Tianjin 300071, P. R. China
E-mail: yuliu@nankai.edu.cn

The ORCID identification number(s) for the author(s) of this article can be found under https://doi.org/10.1002/smll.202101185.

DOI: 10.1002/smll.202101185

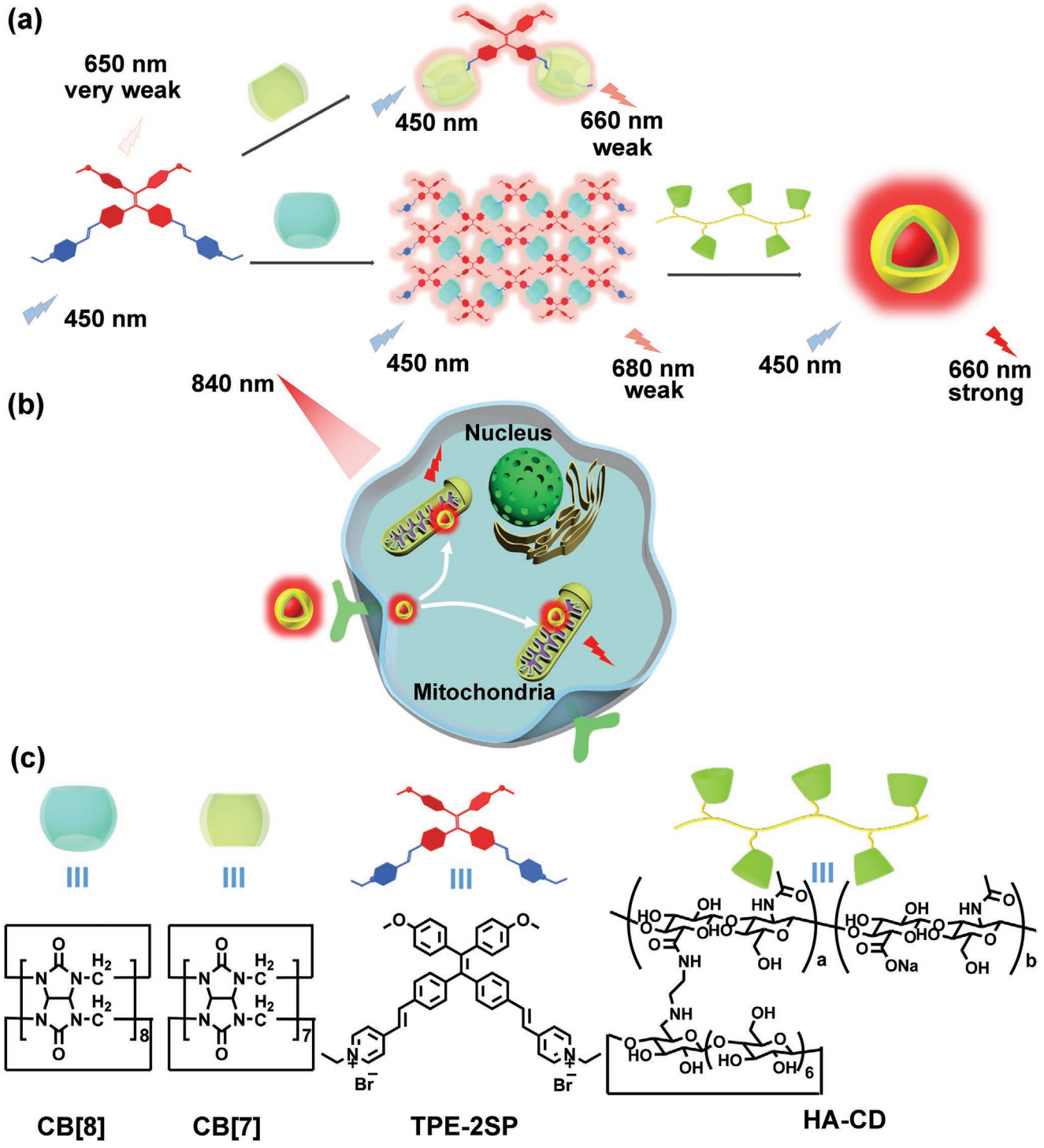

Scheme 1. Schematic Illustration of a) the formation of supramolecular nanoparticle with NIR emission. b) Supramolecular nanoparticle with NIR emission used for two-photon mitochondria targeted imaging of A549 cell. c) Chemical structures of compounds.

Supporting Information). In order to explore the effect of supramolecular macrocyclic compounds on the photochemical property of guest molecule TPE-2SP, CB[8] which has high binding affinity with positively charged pyridinium salts molecules,[17] and β-CD modified hyaluronic acid (HA-CD)[18] which interacts with guest molecules through electrostatic interaction and host–guest interaction were selected as host molecules (Figure S5, Supporting Information).

First, ^{1}H NMR experiment was performed to explore host–guest recognition motif of TPE-2SP and CB[8]. From ^{1}H NMR titration spectra (**Figure 1**a; Figure S6, Supporting Information), upon gradual addition of CB[8], proton peaks related to

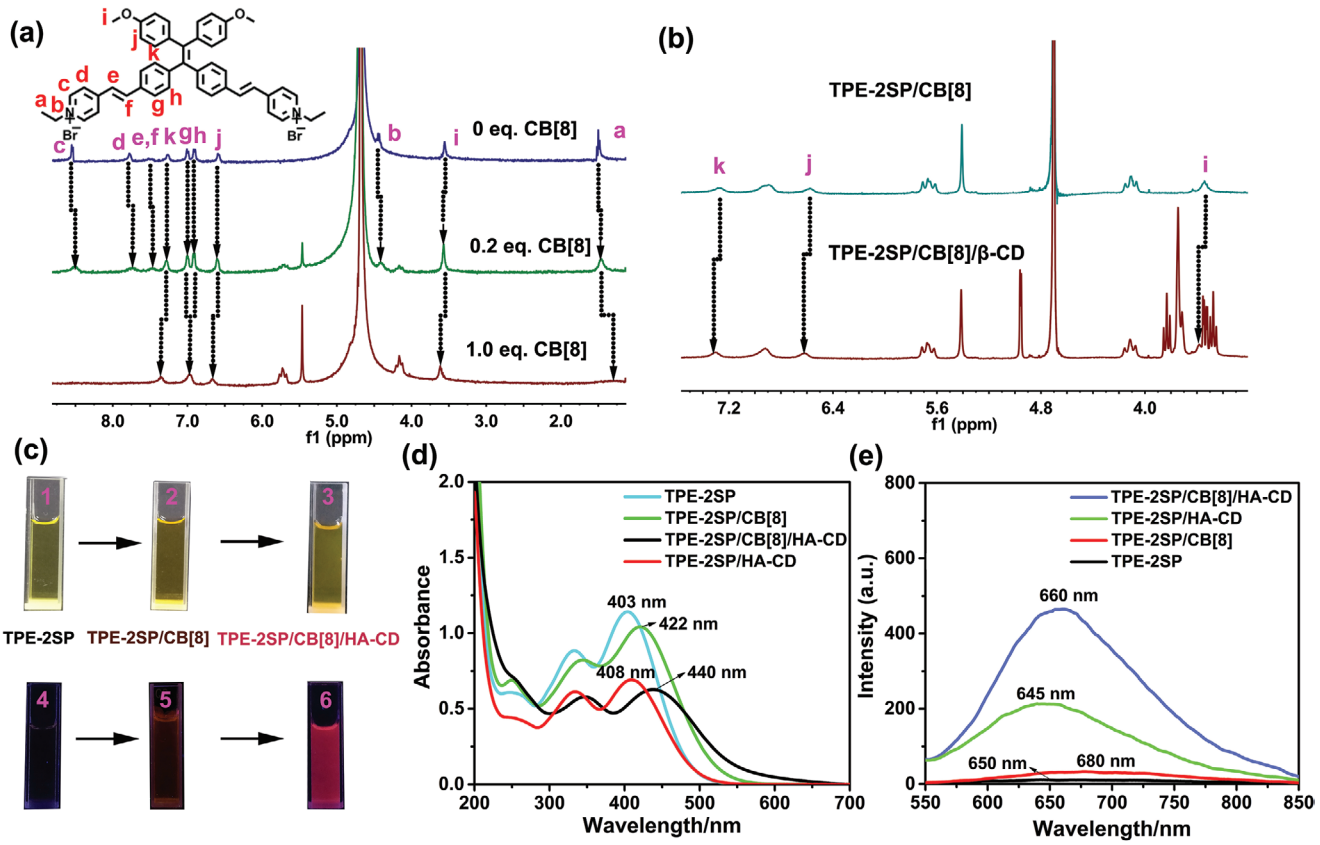

Figure 1. a) ^{1}H NMR spectra (400 MHz, D_2O, 298 K) of TPE-2SP (0.5×10^{-3} M) in the presence of 0.00, 0.20, 1.00 eq. of CB[8]. b) ^{1}H NMR spectra (400 MHz, D_2O, 298 K) of TPE-2SP/CB[8] and TPE-2SP/CB[8]/β-CD ([TPE-2SP] = [CB[8]] = [β-CD] = 0.5×10^{-3} M). c) The photographs of TPE-2SP, TPE-2SP/CB[8], and TPE-2SP/CB[8]/HA-CD aqueous solution under daylight 1–3) and 365 nm UV hand lamp 4–6) at 298 K. d) UV–vis spectra and e) fluorescence spectra of TPE-2SP, TPE-2SP/CB[8], TPE-2SP/CB[8]/HA-CD, and TPE-2SP/HA-CD aqueous solution. ([TPE-2SP] = [CB[8]] = 0.03×10^{-3} M, [HA-CD] = 0.01×10^{-3} M, respectively, λ_{ex} = 450 nm for fluorescence spectra).

H_{a-g} of vinyl pyridinium groups all underwent upfield shifts ($\Delta\delta$ = 0.04, 0.03, 0.05, 0.04, 0.05, and 0.06 ppm for H_a, H_b, H_c, H_d, $H_{e,f}$, and H_g, respectively), indicating these protons were deeply encapsulated into the cavity of CB[8]. Meanwhile, proton signals of H_{h-k} were shifted downfield ($\Delta\delta$ = 0.05, 0.05, 0.07, and 0.08 ppm for H_h, H_i, H_j, and H_k), demonstrating these protons existed close proximity to the portal of CB[8]. Continue to increase the concentration of CB[8] above 1.0 eq., all protons showed no more chemical shifts, implying the stoichiometry ratio of TPE-2SP:CB[8] was 1:1. The Job's plot further conformed to the 1:1 binding stoichiometry between TPE-2SP and CB[8] (Figure S7, Supporting Information). Meanwhile, particular proton signals that shifted upfield disappeared with the increase of CB[8], suggesting the formation of supramolecular polymer in water. Transmission electron microscopy (TEM) and scanning electron microscopy (SEM) provided the evidence of the existence of large-sized supramolecular assemblies. As shown in SEM image (**Figure 2**c), the morphology of TPE-2SP/CB[8] exhibited numerous of nanosquares with a side length range of 200–1000 nm. TEM image further proved the formation of nanosquares morphology (Figure S9a, Supporting Information). On the basis of the above information, a possible assembling mode that two vinyl pyridinium moieties from the adjacent TPE-2SP molecules were simultaneously incorporated into the cavity of CB[8] was proposed (Figure 2a).

Then we studied the spectral properties of TPE-2SP/CB[8] assembly by the use of UV–vis absorption and fluorescence spectroscopy. In the UV–vis absorption spectra (Figure 1d), the maximum absorption peak of TPE-2SP exhibited apparent bathochromic shift from 403 to 422 nm upon the gradual addition of equimolar CB[8] solution, accompanied by a decline of absorbance. Moreover, the color of solution turned from light yellow to dark yellow (Figure 1c). These phenomena may be ascribed to the extension of π-conjugation caused by the formation of stable supramolecular assembly with nanosquares morphology. According to the absorption titration spectra, the association constant (K_a) is determined to be 1.50×10^6 M^{-1} for TPE-2SP/CB[8] in aqueous solution (Figure S10, Supporting Information), indicating that CB[8] has a strong binding ability toward TPE-2SP. As shown in fluorescence spectra (Figure 1e; Figure S12, Supporting Information), TPE-2SP has a very weak fluorescence emission centered at 650 nm, which was enhanced and redshifted to 680 nm upon complexation with CB[8] in water, which may be due to the fact that positively charged pyridinium groups were included into the cavity of CB[8], restricting the rotation of free C=C double bond. Moreover, weak red fluorescence can be observed by naked eyes

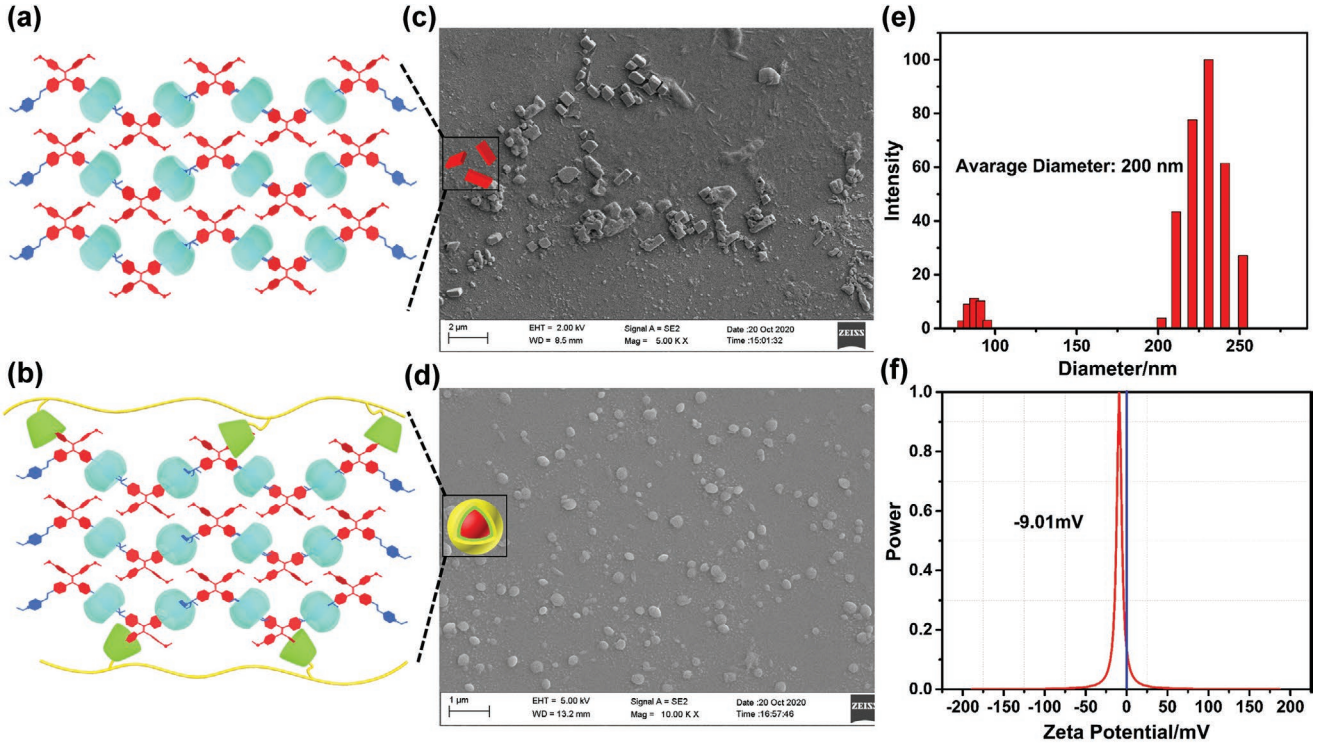

Figure 2. Schematic diagram of a) nanosquare and b) nanoparticle; SEM images of supramolecular assemblies of c) TPE-2SP/CB[8] and d) TPE-2SP/CB[8]/HA-CD; e) DLS data and f) zeta potential of supramolecular nanoparticles TPE-2SP/CB[8]/HA-CD.

under the UV hand lamp at 365 nm illumination (Figure 1c). As comparison, the emission of TPE-2SP also strengthened but only a red shift of 10 nm upon the addition of another macrocycle cucurbit[7]uril (CB[7]) (Figure S12, Supporting Information). It may be due to CB[8] and TPE-2SP can form a tightly packed *n*:*n* polymer, while CB[7] can only form a simple 2:1 complex with TPE-2SP (Figure S8, Supporting Information). According to the previous reports, macrocyclic molecules with high negative charge density such as sulfato-β-cyclodextrin (SCD) or *p*-sulfonatocalix[n]arenes (SCnA) can promote cationic guest molecules to aggregate by the means of electrostatic interaction, enhancing the aggregate stability and compactness, and leading to highly ordered aggregates.[7b,19a] Thus, the negatively charged molecule cancer cell targeting agent β-CD modified hyaluronic acid (HA-CD) was introduced into our current system to induce the secondary assembly of TPE-2SP/CB[8]. In ^{1}H NMR spectra (Figure 1b), the chemical shifts of H_j, H_k, and H_i residing on the methoxybenzene ring of TPE-2SP/CB[8] assembly showed slight downfield shifts ($\Delta\delta$ = 0.05, 0.04, and 0.04 ppm for H_j, H_k, and H_i, respectively) upon the addition of β-CD, indicating β-CD has a certain degree of host–guest complexation on the methoxyphenyl unit of TPE-2SP. Moreover, ^{1}H NMR experiment of TPE-2SP/β-CD was also performed (Figure S13, Supporting Information). With the addition of β-CD, ^{1}H NMR signals related to H_a and H_b protons of vinyl pyridinium groups in TPE-2SP showed no change, while signals related to H_i protons of methoxybenzene ring shifted to downfield, further confirming the inclusion complexation of β-CD with the methoxyphenyl unit of TPE-2SP. The above results are consistent with the previous reports that β-CD can complex neutral guest molecules with aromatic residue.[19b,c] Excitingly, fluorescence titration spectra showed that the NIR fluorescence emission centered at 660 nm of TPE-2SP/CB[8] enhanced significantly upon the gradual addition of HA-CD (Figure S14, Supporting Information), red fluorescence emission can be clearly observed by naked eyes under an ultraviolet lamp (Figure 1c).

According to the optical transmittance changes of TPE-2SP at different concentrations, the critical aggregation concentration (CAC) of TPE-2SP was determined as 0.11×10^{-3} M (Figure S11, Supporting Information). Fixing the concentration of TPE-2SP/CB[8] to 0.03×10^{-3} M, the fluorescence emission was no longer enhanced and reached equilibrium as the concentration of HA-CD was higher than 0.01×10^{-3} M, and the intensity at 660 nm increased by 17-fold than the inherent intensity of TPE-2SP/CB[8] (Figure 1e; Figure S14, Supporting Information), revealing that HA-CD can further restrict the movement of TPE-2SP/CB[8] molecules, and induce the aggregation of TPE-2SP/CB[8] assemblies to promote the NIR emission through electrostatic interaction and host–guest complexation. In control experiments, free TPE-2SP exhibited a similar fluorescence enhancement change like the TPE-2SP/CB[8] upon the addition of HA-CD, and the fluorescence intensity also reached the maximum when the concentration of HA-CD is 0.01×10^{-3} M (Figure 1e; Figure S15, Supporting Information). However, it is worth mentioning that binary supramolecular assembly (TPE-2SP/HA-CD) displayed an emission peak centered at 645 nm and the intensity in the range of 550–800 nm was obviously weaker than that of ternary supramolecular assembly (TPE-2SP/CB[8]/HA-CD). Moreover, the addition order of CB[8] and

HA-CD in ternary supramolecular assembly has almost no effect on luminescence property of guest molecule TPE-2SP (Figure S16, Supporting Information).

In addition, UV–vis absorption spectra showed that the maximum absorption wavelength of TPE-2SP/CB[8] appeared a further bathochromic shift from 420 to 440 nm in the presence of HA-CD, and the absorption range can be extended to 650 nm compared to TPE-2SP/CB[8] (Figure 1d). The color of TPE-2SP/CB[8] aqueous solution under daylight was nearly unchanged in the presence or absent of HA-CD (Figure 1c), indicating that the interaction between HA-CD and TPE-2SP/CB[8] cannot compete the TPE-2SP out of the cavity of CB[8]. On the contrary, mixing TPE-2SP and HA-CD only caused a decrease of the absorbance of TPE-2SP and showed no distinct red shift of maximum absorption peak (Figure 1d). According to these results, CB[8] and HA-CD are both indispensable for the strong near-infrared emission as well as the absorption range expansion of the TPE-2SP. Furthermore, the aggregation behavior of TPE-2SP/CB[8] induced by HA-CD was investigated by Tyndall effect experiment. In the presence of HA-CD, the ternary supramolecular assembly of TPE-2SP/CB[8]/HA-CD aqueous solution showed an obvious Tyndall effect compared to the TPE-2SP/CB[8] binary assembly (Figure S17, Supporting Information), indicating the existence of aggregates. Subsequently, TEM, SEM, and dynamic laser scattering (DLS) were performed to identify the morphology and size characteristics of TPE-2SP/CB[8]/HA-CD ternary assembly. As shown in Figure 2d, SEM image exhibited spherical nanoparticles with the diameter range of 50–300 nm, which is in agreement with the morphology observed in TEM images (Figure S9b, Supporting Information). The size distribution determined by DLS experiment revealed (Figure 2e) that the average diameter of the TPE-2SP/CB[8]/HA-CD nano-particles to be 200 nm, consistent with the diameter measured by SEM and TEM images. Moreover, the zeta potential of supramolecular nanoparticles of TPE-2SP/CB[8]/HA-CD was measured as –9.01 mV (Figure 2f) compared to 8.42 mV of TPE-2SP/CB[8] (Figure S18, Supporting Information). All of these results give the evidence that HA-CD is covered on the surface of the TPE-2SP/CB[8] assembly to form supramolecular nanoparticles through host–guest complexation and electrostatic interactions (Figure 2b). In addition, fluorescence experiment was performed to explore the stability of the supramolecular

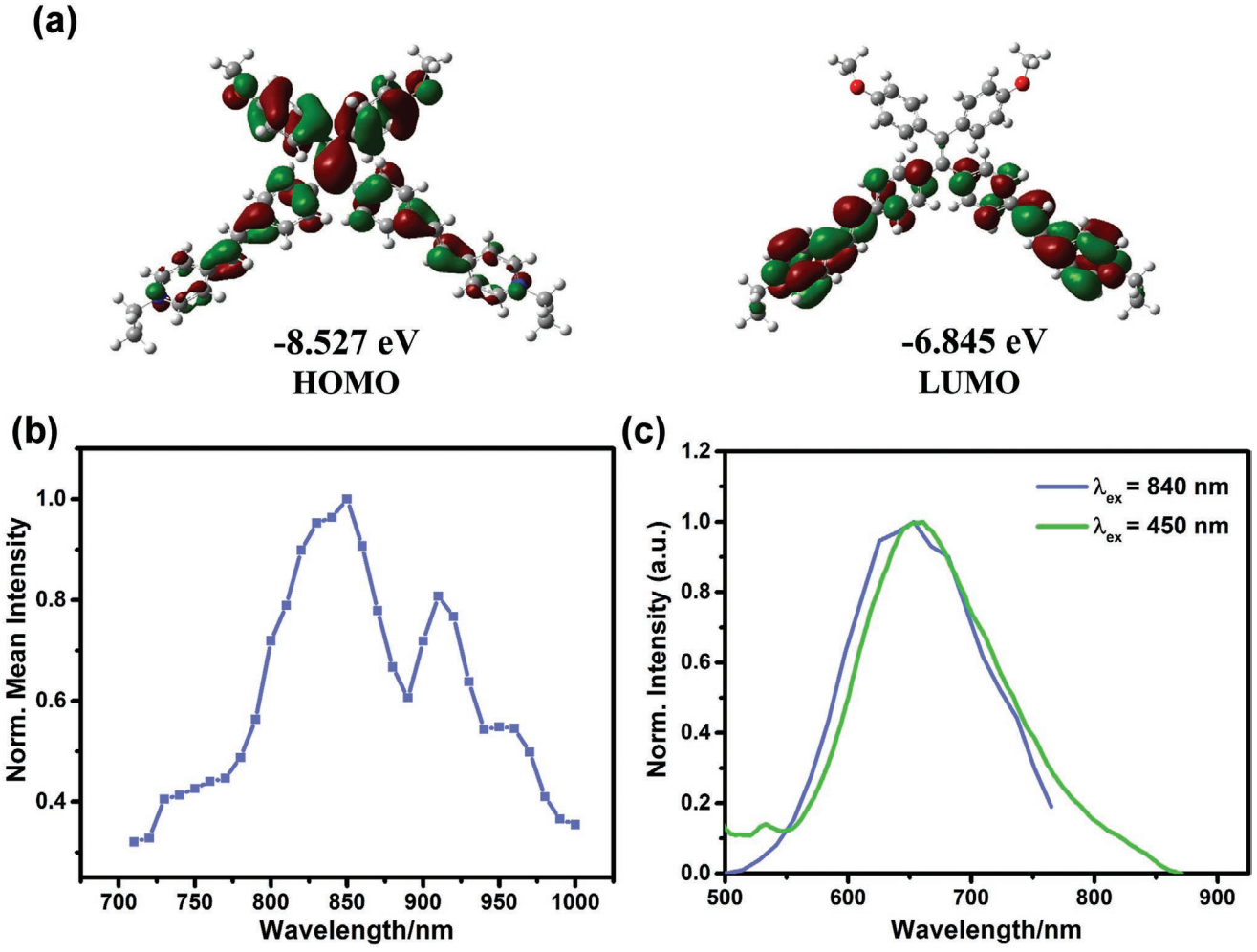

Figure 3. a) HOMO/LUMO orbitals and orbital energies of TPE-2SP-S_0. b) Two-photon excitation spectrum of TPE-2SP/CB[8]/HA-CD in water. c) Emission spectra of supramolecular ternary assembly TPE-2SP/CB[8]/HA-CD excited at 450 nm (green line) and 840 nm (blue line).

nanoparticles. As shown in Figure S19 in the Supporting Information, the fluorescence emission peak and intensity of the nanoparticles measured every 2 h are similar, indicating the good stability of the nanoparticles.

Structurally, the guest molecule TPE-2SP contains methoxyl, TPE, and vinyl pyridine salt groups, displaying a D-conjugated bridge (π)-A type large π conjugate structure. As far as we know, strong push–pull dipolar effect and large conjugation lengths are both conducive to two-photon absorption property. [20] In order to better understand the inherent intramolecular charge transfer (ICT) transitions of TPE-2SP, density functional theory (DFT) calculations, and molecular electrostatic potential (MEP), were performed for TPE-2SP molecule. As illustrated in **Figure 3**a, The HOMO of TPE-2SP-S_0 is mainly localized at the two methoxyphenyl groups, while the LUMO is localized at the two styryl-pyridyl groups, suggesting electron transfer from methoxyphenyl groups to styrene pyridine groups may occur as TPE-2SP is excited. And molecular electrostatic potential (MEP) diagram also gives consistent results (Figure S20, Supporting Information). Therefore, we speculate that the supramolecular assemblies TPE-2SP/CB[8]/HA-CD with strong NIR emission have the property of two-photon absorption. As expected, the excitation wavelength ranges for TPE-2SP/CB[8]/HA-CD is 750–950 nm (Figure 3b). Upon the excitation at 840 nm with femtosecond laser, the fluorescence spectrum of TPE-2SP/CB[8]/HA-CD showed similar spectral band and position with one-photon excitation at 450 nm (Figure 3c), endowing the supramolecular nanoparticles with features of higher penetrability for cells and lower phototoxicity. In addition, HA-CD on the surface of supramolecular nanoparticles renders supramolecular ternary assembly the capability to target cancer cells. [18,21] Benefiting from the above functional characteristics of the supramolecular ternary assembly TPE-2SP/CB[8]/HA-CD, we applied it to the targeted imaging of cancer cells. Human lung adenocarcinoma cells (A549 cells) were treated with TPE-2SP/CB[8]/HA-CD nanoparticles for 8 h, and A549 cells were co-stained with mitochondria staining dye Mito-Tracker Green and TPE-2SP/CB[8]/HA-CD nanoparticles. Subsequently, the two-photon and confocal laser scanning microscopy (CLSM) experiments were performed to investigate the intracellular distribution. As shown in **Figure 4**a,d, red luminescence can be observed in cell cytoplasm when excited by 405 nm laser as well as 840 nm femtosecond pulsed laser, and the merged yellow dyeing sites of red TPE-2SP/CB[8]/HA-CD and green Mito-Tracker as well as the high Pearson's co-efficient of mito-targeting effect demonstrated that the nanoparticles can target mitochondria in A549 cells (Figure 4b,c,e,f and Figure S21, Supporting Information). Evidently, the NIR light irradiation allows for using the TPE-2SP/CB[8]/HA-CD supramolecular nanoparticles with NIR emission in biological targeting imaging system. Moreover, the cytotoxicity experiments were carried out in A549 cells by CCK-8 assays. The viability results shown in Figure S22 in the Supporting Information demonstrated the nanoparticles were less toxic to A549 cells.

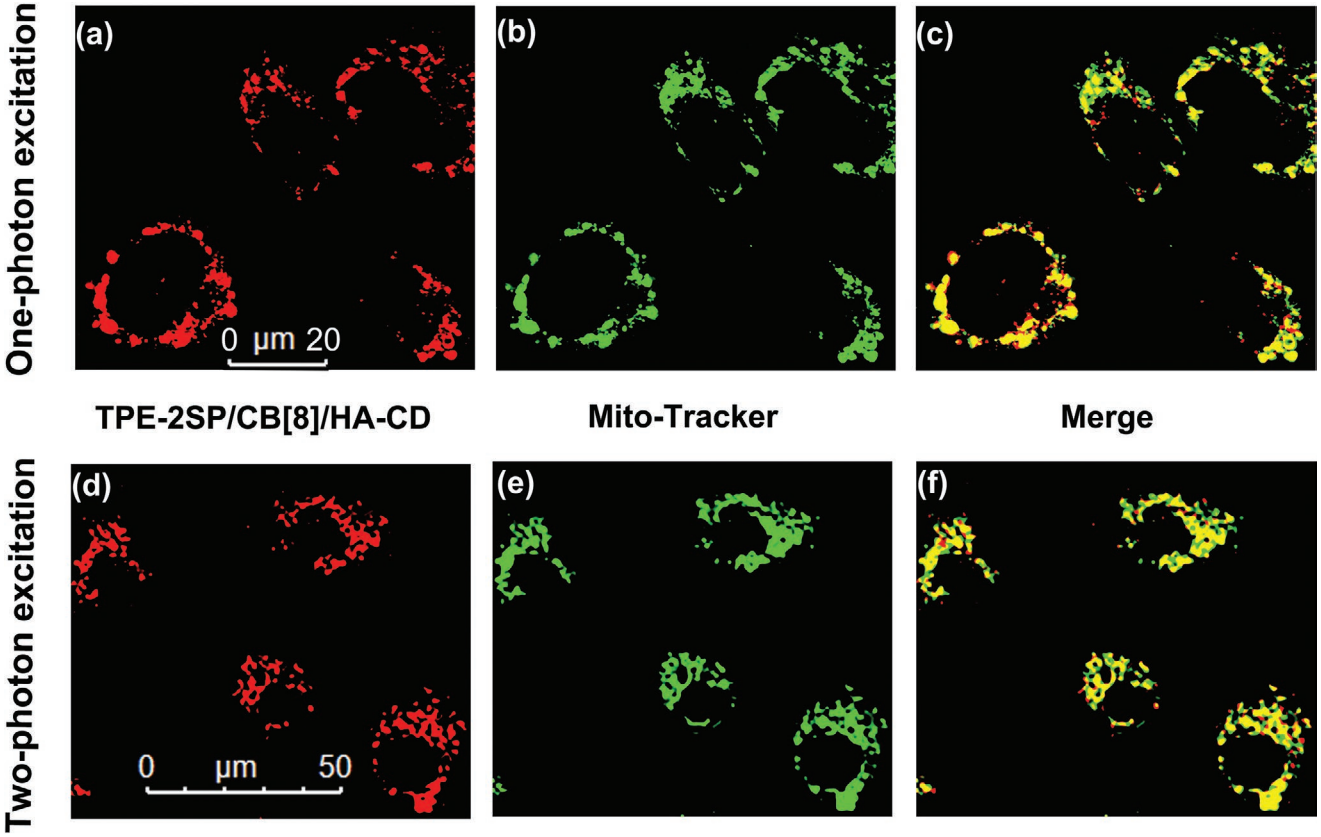

Figure 4. CLSM images of A549 cells incubated with a) TPE-2SP/CB[8]/HA-CD ([TPE-2SP] = 0.005×10^{-3} M) excited at 405 nm. b) Mito-Tracker Green and c) the merged image of (a,b); Two-photon microscopic images of A549 cells incubated with d) TPE-2SP/CB[8]/HA-CD ([TPE-2SP] = 0.005×10^{-3} M) excited at 840 nm. e) Mito-Tracker Green and f) The merged image of (d,e).

3. Conclusion

In conclusion, we present supramolecular NIR emission nanoparticles with two-photon for cancer cell targeting imaging. In this system, the guest molecule TPE-2SP used as a basic building block, which interacted with the macrocyclic molecules cucurbit[7, 8]uril (CB[7,8]), leading to host–guest induced increase of near-infrared emission. Moreover, TPE-2SP/CB[8] was more than 20 nm redshift than TPE-2SP/CB[7]. Intriguingly, the NIR emission strengthened after adding HA-CD to further assemble with TPE-2SP/CB[8] to form supramolecular nanoparticles. This new supramolecular assembly system solves the short wavelength excitation and emission problems of previous supramolecular imaging systems, exhibits the advantages of low phototoxicity, deep tissue penetration and high imaging quality, and opens up new ideas for the application of supramolecular systems in biology, especially cell imaging.

Supporting Information

Supporting Information is available from the Wiley Online Library or from the author.

Acknowledgements

This work was supported by National Natural Science Foundation of China (Grants 21971127, 21772099, and 21861132001). The cell image acquisition was supported by Biological Imaging and Analysis Laboratory, Medical and Healthy Analytical Center, Peking University, especially Jing Wu.

Conflict of Interest

The authors declare no conflict of interest.

Data Availability Statement

The data that support the findings of this study are available on request from the corresponding author.

Keywords

mitochondrial targeted imaging, near-infrared emission, supramolecular assembly, two-photon absorption

Received: February 28, 2021
Revised: April 2, 2021
Published online: June 18, 2021

[1] J. Luo, Z. Xie, J. W. Y. Lam, L. Cheng, H. Chen, C. Qiu, H. S. Kwok, X. Zhan, Y. Liu, D. Zhu, B. Z. Tang, *Chem. Commun.* **2001**, *18*, 1740.
[2] a) T. Wang, X. Su, X. Zhang, X. Nie, L. Huang, X. Zhang, X. Sun, Y. Luo, G. Zhang, *Adv. Mater.* **2019**, *31*, 1904273; b) H. Ding, J. Li, G. Xie, G. Lin, R. Chen, Z. Peng, C. Yang. B. Wang, J. Sun, C. Wang, *Nat. Commun.* **2018**, *9*, 5234.
[3] R. Zhang, Y. Duan, B. Liu, *Nanoscale* **2019**, *11*, 19241.
[4] a) Q. Zhang, P. Yu, Y. Fan, C. Sun, H. He, X. Liu, L. Lu, M. Zhao, H. Zhang, F. Zhang, *Angew. Chem., Int. Ed.* **2021**, *60*, 3967; b) F. Würthner, *Angew. Chem., Int. Ed.* **2020**, *59*, 14192.
[5] J.-L. Liu, J.-Q. Zhang, Z.-L. Tang, Y. Zhuo, Y.-Q. Chai, R. Yuan, *Chem. Sci.* **2019**, *10*, 4497.
[6] D. Dai, Z. Li, J. Yang, C. Wang, J.-R. Wu, Y. Wang, D. Zhang, Y.-W. Yang, *J. Am. Chem. Soc.* **2019**, *141*, 4756.
[7] a) Y. Li, Y. Dong, X. Miao, Y. Ren, B. Zhang, P. Wang, Y. Yu, B. Li, L. Isaacs, L. Cao, *Angew. Chem., Int. Ed.* **2018**, *57*, 729; b) Z. Liu, X. Dai, Y. Sun, Y. Liu, *Aggregate* **2020**, *1*, 31.
[8] H.-T. Feng, Y.-X. Yuan, J.-B. Xiong, Y.-S. Zheng, B. Z. Tang, *Chem. Soc. Rev.* **2018**, *47*, 7452.
[9] J. Mosquera, Y. Zhao, H.-J. Jang, N. Xie, C. Xu, N. A. Kotov, L. M. Liz-Marzán, *Adv. Funct. Mater.* **2020**, *30*, 1902082.
[10] a) C. Stoffelen, J. Huskens, *Small* **2016**, *12*, 96; b) X. Ma, J. Wang, H. Tian, *Acc. Chem. Res.* **2019**, *52*, 738; c) B. Shi, K. Jie, Y. Zhou, J. Zhou, D. Xia, F. Huang, *J. Am. Chem. Soc.* **2016**, *138*, 80.
[11] a) T. Kim, J. Y. Park, J. Hwang, G. Seo, Y. Kim, *Adv. Mater.* **2020**, *32*, 2002405; b) X.-M. Chen, Y. Chen, Q.-L. Yu, B.-H. Gu, Y. Liu, *Angew. Chem., Int. Ed.* **2018**, *57*, 12519.
[12] J. Li, J. Wang, H. Li, N. Song, D. Wang, B. Z. Tang, *Chem. Soc. Rev.* **2020**, *49*, 1144.
[13] a) T. L. Mako, J. M. Racicot, M. Levine, *Chem. Rev.* **2019**, *119*, 322; b) F.-F. Shen, Y.-M. Zhang, X.-Y. Dai, H.-Y. Zhang, Y. Liu, *J. Org. Chem.* **2020**, *85*, 6131.
[14] M. Pawlicki, H. A. Collins, R. G. Denning, H. L. Anderson, *Angew. Chem., Int. Ed.* **2009**, *48*, 3244.
[15] a) Y. Shen, A. J. Shuhendler, D. Ye, J.-J. Xu, H.-Y. Chen, *Chem. Soc. Rev.* **2016**, *45*, 6725; b) L. Wu, J. Liu, P. Li, B. Tang, T. D. James, *Chem. Soc. Rev.* **2021**, *50*, 702.
[16] a) H. Li, Q. Yao, J. Fan, J. Du, J. Wang, X. Peng, *Biosens. Bioelectron.* **2017**, *94*, 536; b) Z. Zheng, D. Li, Z. Liu, H.-Q. Peng, H. H. Y. Sung, R. T. K. Kwok, I. D. Williams, J. W. Y. Lam, J. Qian, B. Z. Tang, *Adv. Mater.* **2019**, *31*, 1904799.
[17] a) C. Hu, Y. Lan, K. R. West, O. A. Scherman, *Adv. Mater.* **2015**, *27*, 7957; b) L. Isaacs, *Acc. Chem. Res.* **2014**, *47*, 2052.
[18] a) F.-Q. Li, Q.-L. Yu, Y.-H. Liu, H.-J. Yu, Y. Chen, Y. Liu, *Chem. Commun.* **2020**, *56*, 3907.
[19] a) J.-J. Li, Y. Chen, J. Yu, N. Cheng, Y. Liu, *Adv. Mater.* **2017**, *29*, 1701905; b) L. Leclercq, N. Noujeim, S. H. Sanon, A. R. Schmitzer, *J. Phys. Chem. B* **2008**, *112*, 14176; c) X. Ma, J. Cao, Q. Wang, H. Tian, *Chem. Commun.* **2011**, *47*, 3559.
[20] Y. Li, S. Liu, H. Ni, H. Zhang, H. Zhang, C. Chuah, C. Ma, K. S. Wong, J. W. Y. Lam, R. T. K. Kwok, J. Qian, X. Lu, B. Z. Tang, *Angew. Chem., Int. Ed.* **2020**, *59*, 12822.
[21] F.-F. Shen, Y. Chen, X. Dai, H.-Y. Zhang, B. Zhang, Y. Liu, Y. Liu, *Chem. Sci.* **2021**, *12*, 1851.